J. Fluid Mech. (1972), *vol.* 51, *part* 1, *pp.* 39–61
Printed in Great Britain

Numerical studies of the stability of inviscid stratified shear flows

By PHILIP HAZEL

Department of Applied Mathematics and
Theoretical Physics, Cambridge†

(Received 21 August 1970 and in revised form 6 August 1971)

The infinitesimal stability of inviscid, parallel, stratified shear flows to two-dimensional disturbances is described by the Taylor–Goldstein equation. Instability can only occur when the Richardson number is less than $\frac{1}{4}$ somewhere in the flow. We consider cases where the Richardson number is everywhere non-negative. The eigenvalue problem is expressed in terms of four parameters, J a 'typical' Richardson number, α the (real) wavenumber and c the complex phase speed of the disturbance. Two computer programs are developed to integrate the stability equation and to solve for eigenvalues: the first finds c given α and J, the second finds α and J when $c \equiv 0$ (i.e. it computes the stationary neutral curve for the flow). This is sometimes, *but not always*, the stability boundary in the α, J plane. The second program works only for cases where the velocity and density profiles are antisymmetric about the velocity inflexion point. By means of these two programs, several configurations of velocity and density have been investigated, both of the free-shear-layer type and the jet type. Calculations of temporal growth rates for particular profiles have been made.

1. Introduction

The stability equation for small disturbances in an inviscid, incompressible, stratified, parallel shear flow, when the Boussinesq approximation is made, is

$$\frac{d^2w}{dz^2} + \left\{\frac{N^2(z)}{(U(z)-C)^2} - \frac{d^2U/dz^2}{U(z)-C} - k^2\right\} w(z) = 0, \tag{1.1}$$

where $w(z)$ is a single Fourier component of the vertical perturbation velocity, z is the vertical co-ordinate, $N(z)$ is the local Brunt–Väisälä frequency, given by $N^2(z) = -g(d\rho/dz)/\rho$; $U(z)$ is the basic velocity profile and C is the complex phase speed of the wave mode of wavenumber k; $k\,\mathrm{Im}\,(C)$ thus represents a growth (or decay) rate of the waves. Derivations of (1.1) are given by Miles (1961), and Drazin & Howard (1966); Thorpe (1969) proposed that (1.1) be called the Taylor–Goldstein equation, because Taylor (1931) and Goldstein (1931) first derived it. Together with suitable boundary conditions, it defines an eigenvalue problem for C given k, or vice versa. We shall consider flows with rigid, horizontal boundaries; mathematically this means setting $w(\pm z_b) = 0$, where z_b is the distance of the boundaries from the origin, possibly infinite.

† Present address: Computer Laboratory, Corn Exchange Street, Cambridge CB 2 3QG.

The Taylor–Goldstein equation is usually considered in a dimensionless form, but there are slight differences in the ways different authors achieve the non-dimensionalization. This can lead to misunderstandings in effecting comparisons. We shall use the following scheme for non-dimensionalizing (1.1). (i) Let the dimensionless vertical co-ordinate be $y = z/h$, where h is some 'typical' height. (ii) Let the dimensionless wavenumber be $\alpha = kh$. (iii) Choose axes such that $U(0) = 0$ (we shall, in fact, be placing the origin at the inflexion point of the velocity profile), then write

$$U(y) = Vu(y) \quad \text{such that} \quad (du/dy)_{y=0} = 1,$$

$$\log(\rho_0/\rho) = \lambda(y) = \sigma\beta(y) \quad \text{such that} \quad (d\beta/dy)_{y=0} = 1.$$

Thus V is a typical velocity, σ a typical density measure. (iv) Let the dimensionless complex phase velocity be $c = C/V$. On this scaling, the Brunt–Väisälä frequency is given by

$$N^2(y) = g\frac{d\lambda}{dz} = \sigma g\frac{d\beta}{dy}\Big/h. \tag{1.2}$$

The local Richardson number is

$$Ri(y) = \frac{N^2(y)}{(dU/dz)^2} = \frac{J\,d\beta/dy}{(du/dy)^2}, \tag{1.3}$$

where $J = \sigma gh/V^2$, while the dimensionless Taylor–Goldstein equation is

$$\phi'' + \left\{\frac{J\beta'}{(u-c)^2} - \frac{u''}{u-c} - \alpha^2\right\}\phi(y) = 0, \tag{1.4}$$

where the dash means d/dy, and ϕ is the dimensionless form of w. We shall adopt the notation that $c = c_r + ic_i$. As ϕ is periodic in the x direction, it is directly proportional to the streamfunction, which therefore satisfies the same equation.

The use of this particular scaling for U and ρ ensures that the dimensionless number J is always equal to the local Richardson number *at the origin*. This we shall take as a Richardson number for the flow. Although in some cases this is somewhat unphysical, it has the merit of uniformity for comparisons between different cases.

Eigensolutions of (1.4) with $c_i > 0$ represent unstable wave modes with growth rate αc_i. Those with $c_i < 0$ represent decaying modes. By taking the complex conjugate of (1.4), it is at once seen that, if $\phi = \psi$ is a solution with eigenvalue $c = \gamma$ (say), then $\phi = \psi^*$ is also a solution, with eigenvalue $c = \gamma^*$. Hence, the eigenvalues always appear in pairs, with one growing and one decaying mode, except when $c_i = 0$, when there is only one, the neutral mode. However, the appearance of the decaying mode is due to the fact that we are using the inviscid equations. In practice, it would not be expected to appear, and it will be ignored in the rest of this paper. If the velocity and density profiles are both anti-symmetric about the origin, another solution can be easily found, namely $\phi = \psi$, $c = -\gamma^* = -\gamma_r + i\gamma_i$. Thus, in these cases of anti-symmetry, unstable modes always appear in pairs of equal growth rate, travelling in opposite directions with equal phase speeds.

We can now summarize some important theorems.

(i) A sufficient condition for stability is $Ri(y) > \frac{1}{4}$ everywhere in the flow (Miles 1961; Howard 1961).

(ii) For given α and J, unstable eigenvalues of c (i.e. with $c_i > 0$) must lie in a semicircle in the c plane, based on the range of $u(y)$ (Howard 1961).

(iii) The existence of a singular neutral mode (SNM), i.e. a mode with $c_i = 0$ and c_r within the range of $u(y)$, implies the existence of contiguous unstable modes (Miles 1963).

(iv) The 'neutral curve' $J = J_0(\alpha)$, which is the locus of SNM's in the α, J plane, is not in general single-valued. Each branch corresponds to a distinct SNM (Miles 1963).

(v) The principle of 'exchange of stabilities' holds for a *stationary* SNM ($c_r = c_i = 0$) if $u'(y)$ and $\beta'(y)$ are positive definite functions *of* u that possess analytic continuation into the complex u plane (Miles 1963).

These theorems have formed the basis of previous analytic investigations. One of the most important physical aspects of the problem is determining the stability boundary of any given configuration in the α, J plane. As theorem (iii) states, if a SNM can be found, then at least one unstable mode exists. However, nothing can be said in general as to whether the associated neutral curve is a stability boundary or not. Theorem (v), although appearing to remove this difficulty in the case of stationary SNM's, is in fact of limited application, because of the restrictions on β' as a function of u. Only a few configurations satisfy the required conditions.

2. Presentation of results

A number of different configurations of velocity and density profiles have been investigated numerically, using two programs that are fully described in the appendix. The velocity profiles can be divided into three classes: shear layers, channel profiles, and jet profiles. Here follows a short summary of the notation, and a brief description of the programs. All variables are dimensionless.

2.1. *Notation*

y is the vertical co-ordinate; $u(y)$ is the basic velocity profile, normalized so that $u(0) = 0$, $u'(0) = 1$; $\beta(y)$ is the basic density profile, in the form $\log(\rho_0/\rho)$, normalized so that $\beta'(0) = 1$. x is the horizontal co-ordinate, α the wavenumber; J is the Richardson number at the origin, $Ri(y)$ the Richardson number distribution, and $J_0(\alpha)$ is the neutral curve in the α, J plane. $c = c_r + ic_i$ is the complex phase speed of waves; αc_i is the growth rate of unstable waves; $\phi(y)$ is the vertical perturbation velocity for the mode of wavenumber α.

2.2. *Programs*

(i) The first program computes the value of c for given profiles, given α and J, if an unstable eigenvalue exists. If not, then either the solution is neutral, or there is no solution. The program cannot distinguish between these two cases. (ii) The second program computes stationary neutral curves in the α, J plane for con-

figurations where both the velocity and the density are antisymmetric in y. It cannot determine whether these curves are stability boundaries or not; this information can, however, be obtained by careful use of program (i). All results were computed to an accuracy of four significant figures.

3. Shear layers

3.1. *The hyperbolic tangent shear layer*

The velocity profile $u(y) = \tanh(y)$ is important, because it is the prototype of smooth shear layers. We consider it in conjunction with the density profile $\beta(y) = \tanh(y)$. The neutral curve and stability boundary for this configuration is $J_0 = \alpha(1-\alpha)$ (Holmboe 1960), which is a parabola symmetric about $\alpha = 0{\cdot}5$. Within the unstable region, a large number of eigenvalues of c have been computed, and from this data the maximum growth rates for given J can be deduced by interpolation. Figure 1 shows the neutral curve and the curve of maximum growth. The unstable waves that one would expect to see in an experimental situation are those with the fastest growth rate, for given J.

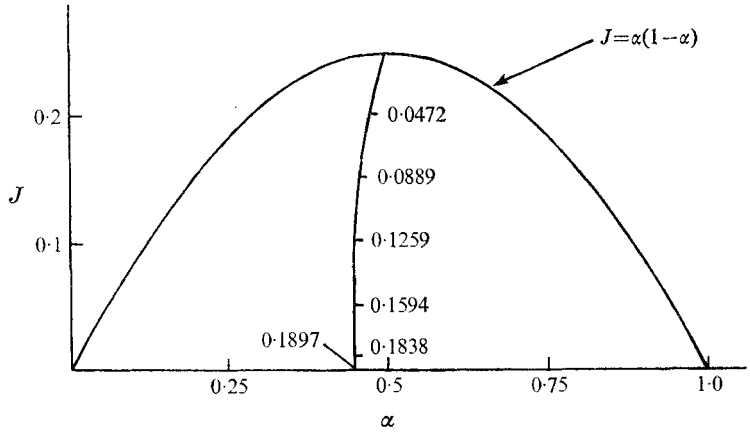

FIGURE 1. Stability boundary and curve of maximum growth rate for 'tanh' profiles, with growth rates marked.

A convenient way of presenting eigenfunctions, which brings out their structure more clearly, is to draw displacements of initially horizontal lines in the flow, after some arbitrary time, chosen so that the amplitudes are not so large as to completely vitiate infinitesimal theory. The dimensionless displacement at any point is given by

$$d(x,y) = \mathrm{Re}\left\{\frac{\phi(y)\exp\{i\alpha(x-ct)\}}{u(y)-c}\right\}, \tag{3.1}$$

and is easily computed from ϕ. Figure 2 is a picture of such displacements; the lines are initially equally spaced. They may be thought of as dye lines in the fluid, or as constant density surfaces, noting that the difference in density between pairs of line varies from pair to pair. The area shown covers one and a quarter wavelengths in the x direction, and, in the y direction, that part of the flow which contains the major part of the disturbance. The velocity profile is shown for

reference on the left; the top and bottom horizontal lines are drawn for reference, and are not part of the flow. The diagram is drawn correctly to scale, i.e. one unit in the x direction is drawn the same length as one unit in the y direction, and it clearly demonstrates the structure of the disturbance.

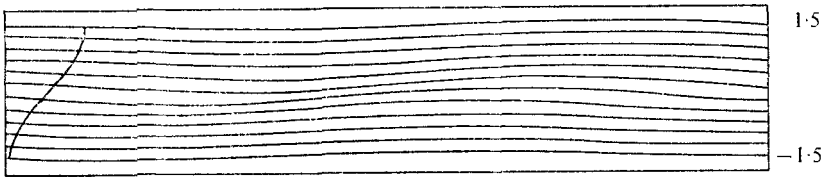

FIGURE 2. Displacement of dye lines in 'tanh' shear flow, with $\alpha = 0{\cdot}4449$ and $J = 0{\cdot}05$.

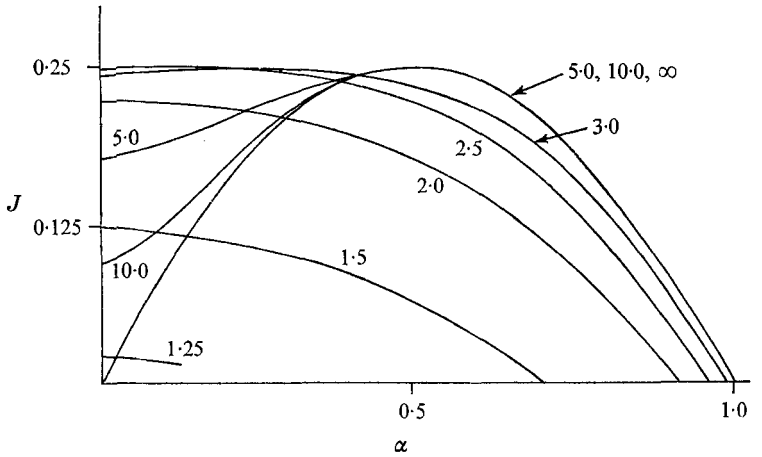

FIGURE 3. Stability boundaries for 'tanh' profiles, with rigid boundaries at distances marked.

3.11. *Effect of boundaries.* When the boundaries of the flow are not at infinity, the shape of the neutral curve, and also the stability characteristics, are altered. Figure 3 shows the changes in the position of the neutral curve (given by program (ii)) for boundaries at different distances. Tests with program (i) establish that it remains the stability boundary. As the boundaries are moved in from infinity, two effects are noticed. The longer wavelengths are de-stabilized, and the left-hand branch of the curve rises, while the shorter wavelengths become more stable (for given J) causing the right-hand branch to move to the left. Eventually, the latter effect dominates, and, for boundaries closer than a critical distance apart, the flow is stable for all α and J.

Howard (1964) has investigated the effect of boundaries on a homogeneous hyperbolic tangent shear layer, and has found the critical distances at which the flow becomes stable for all wavelengths to be given by $y_{\text{crit}} = 1{\cdot}1997$. Using program (ii), it was not found possible to determine y_{crit} in the stratified case better than $1{\cdot}195 < y_{\text{crit}} < 1{\cdot}205$, owing to numerical instabilities that arise when

both α and J are small. However, the agreement with Howard's figure is good. The value of y_{crit} should be the same as in the homogeneous case, as it is a limit with J tending to zero.

The initial destabilization of the longer wavelengths for non-zero Richardson number is at first sight an unexpected result. The mechanism can be understood by considering a two-fluid system between walls, with constant density and

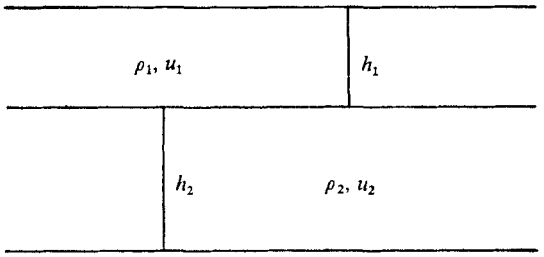

FIGURE 4

velocity in each fluid (see figure 4). A well-known result for interfacial waves is that the wavenumber k is given (in dimensional form) by

$$g(\rho_2-\rho_1) = k\rho_1(u_1-c)^2\coth(kh_1)+k\rho_2(u_2-c)^2\coth(kh_2). \tag{3.2}$$

Consider long waves, keeping h_1 and h_2 finite. Then

$$g(\rho_2-\rho_1) \cong \frac{\rho_1(u_1-c)^2}{h_1}+\frac{\rho_2(u_2-c)^2}{h_2} \tag{3.3}$$

for kh_1 and $kh_2 \ll 1$. We make the Boussinesq approximation, and write

$$\rho_1 \sim \rho_2 = \rho.$$

Also, for simplicity, write $u_1 = -u_2 = V$, $h_1 = h_2 = h$, and $(\rho_2-\rho_1)/\rho = 2\sigma$. Then

$$2\sigma gh = 2(V^2+c^2). \tag{3.4}$$

Thus, the flow is unstable if $\sigma gh/V^2 < 1$, and a decrease in h can cause the flow to be destabilized.

Now, in the case of the hyperbolic tangent shear layer, when Y, the distance of the boundaries from the origin, is greater than about 2.7 (the point at which $\tanh Y \cong 0{\cdot}99$), the configuration will behave for long waves in the same way as the two-layer system we have just discussed, since the ranges of u and ρ remain approximately constant, and independent of Y. Thus, we expect long waves to be destabilized by decreasing Y. However, when Y is less than about 2·7, the ranges of u and ρ decrease with Y, and the system ceases to resemble a two-fluid system for long waves, tending to uniform shear and linear density. In this case, therefore, we would expect unstable long waves to be eventually stabilized by decreasing Y. Referring to figure 3 we see that the point where the left-hand branch of the stability boundary starts to descend again is approximately at $Y = 2{\cdot}5$.

3.12. *Effects of change of density scale.* Since in most laboratory experiments and naturally occurring situations the vertical scales of the velocity and density shear

layers are in general different, the effect of changing the density scale with respect to the velocity scale was investigated, using the following configurations:

$$u(y) = \tanh(y), \quad \beta(y) = (1/R)\tanh(Ry) \quad (-\infty \leqslant y \leqslant \infty), \tag{3.5}$$

where R is the ratio of the scales. As R tends to infinity, the density structure tends to a step, of zero width. The Richardson number distribution for this configuration is

$$Ri(y) = \frac{J\cosh^4(y)}{\cosh^2(Ry)}. \tag{3.6}$$

Ri/J is shown for different values of R in figure 5. The stationary neutral curves for this configuration (for different values of R) are shown in figure 6, while the value of α at the maximum of the neutral curve (which is always at $J = \frac{1}{4}$) is

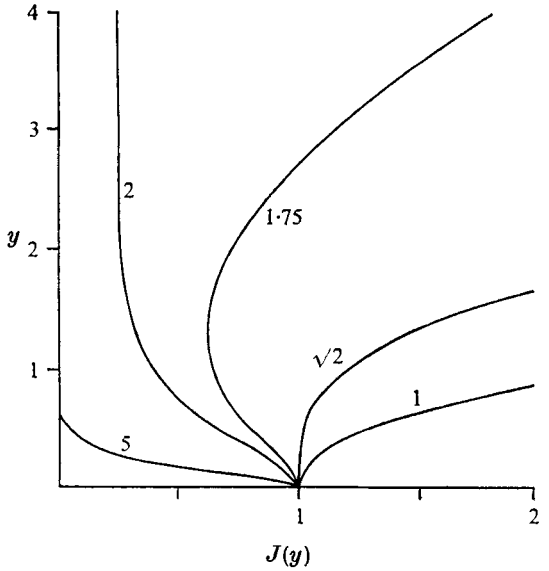

FIGURE 5. Richardson number profiles $Ri(y)/J$ for $u = \tanh(y)$, $\beta = \tanh(Ry)/R$, as R varies.

shown plotted against R in figure 7. This is the wavenumber that would be expected to become unstable first, with decreasing J, in cases where the stationary neutral curves are stability boundaries.

In investigating the stability characteristics, we shall consider separately the three different kinds of Richardson number profile.

(i) For $0 \leqslant R \leqslant \sqrt{2}$, $Ri(y)$ has a minimum at $y = 0$, and is monotonically increasing to infinity as $y \to \pm\infty$. As $R = 1$ falls in this régime, we expect that other values will give similar characteristics, viz. a stability boundary which is a stationary neutral curve. The case $R = 0{\cdot}5$ was briefly considered; outside the neutral curve program (i) would not converge, while the growth rates obtained inside it tend to zero on the curve, as expected.

(ii) For $\sqrt{2} \leqslant R \leqslant 2$, $Ri(y)$ has a local *maximum* at $y = 0$, with minimum at $y = \pm y_{\min}$ (given by $2\tanh y_{\min} = R\tanh Ry_{\min}$), but still tends to infinity as

$y \to \pm\infty$. The cases $R = 1{\cdot}75$ and $R = 2{\cdot}0$ were investigated, using program (i). The only unstable solutions found were inside the stationary neutral curves, and the growth rates decrease to zero as they are approached. We conclude that the stationary neutral curve is the stability boundary in this régime also.

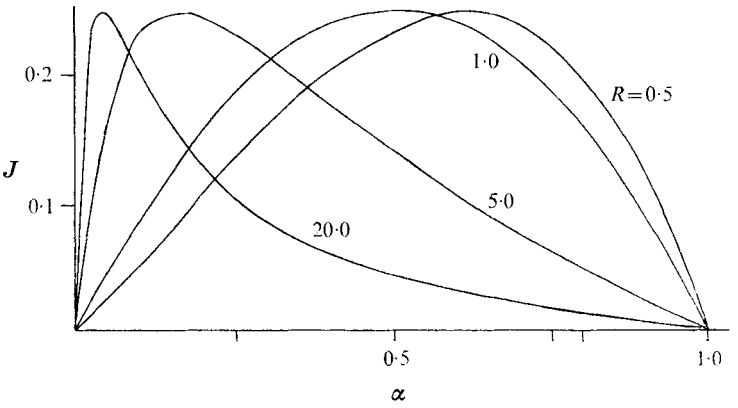

FIGURE 6. Stationary neutral curves for $u = \tanh(y)$, $\beta = \tanh(Ry)/R$, R values as marked.

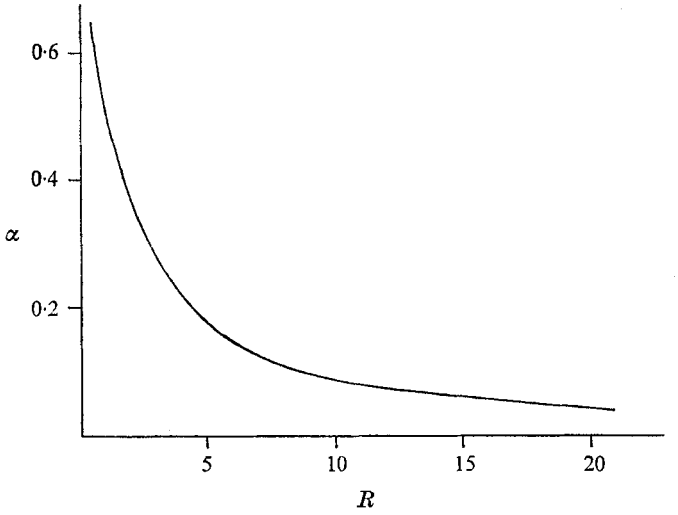

FIGURE 7. Values of α giving $J = 0{\cdot}25$ on the stationary neutral curves as a function of R, for $u = \tanh(y)$, $\beta = \tanh(Ry)/R$.

(iii) For $R > 2$, $Ri(y)$ tends to *zero* as $y \to \pm\infty$, and J is its *maximum* value. The case $R = 5{\cdot}0$ has been thoroughly investigated, and several interesting features have appeared. The stationary neutral curve is not the stability boundary, and an anomalous modal structure exists. The stability characteristics are summarized in figures 8 (a, b), in which the various regions are as follows. (a) In these regions, program (i) finds no unstable solutions. The only possible solutions are therefore neutral ones. (b) In this region, an unstable moving mode is found ($c_r \neq 0, c_i > 0$). Because of the anti-symmetry of the velocity and density profiles,

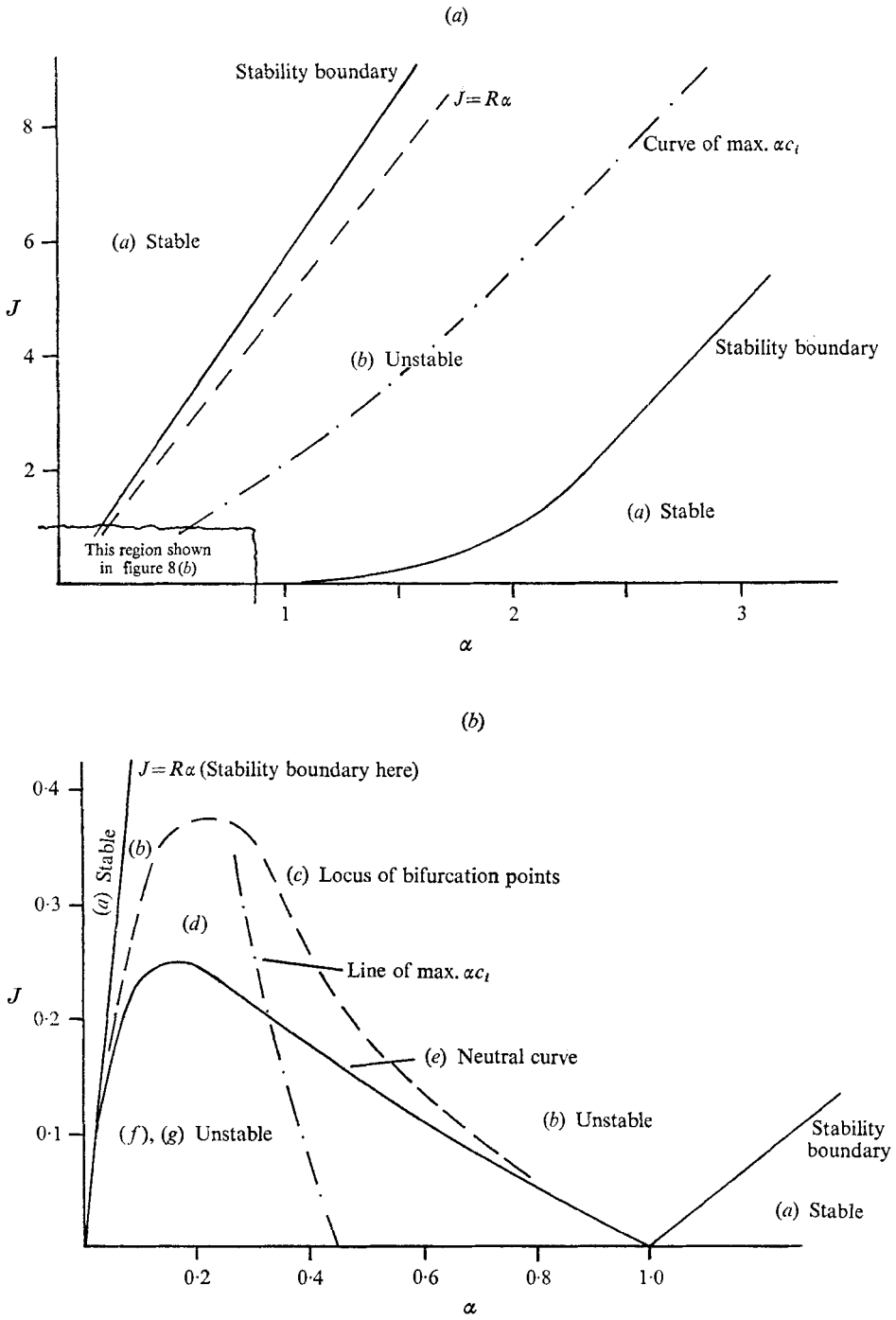

FIGURE 8. (*a*) Approximate stability characteristics for $u = \tanh(y)$, $\beta = \tanh(Ry)/R$, with $R = 5$. (*b*) A portion of (*a*) with the J scale much expanded.

there are in fact two modes, of the same growth rate, moving with equal velocity in opposite directions. (*d*) In this region, there are *two* stationary, unstable modes ($c_r = 0$, $c_i > 0$). The dividing line (*c*), between regions (*b*) and (*d*), marks the locus of bifurcation points in the c plane, points where the phase velocities of the two modes of region (*b*) become zero, and the growth rates of all four modes of

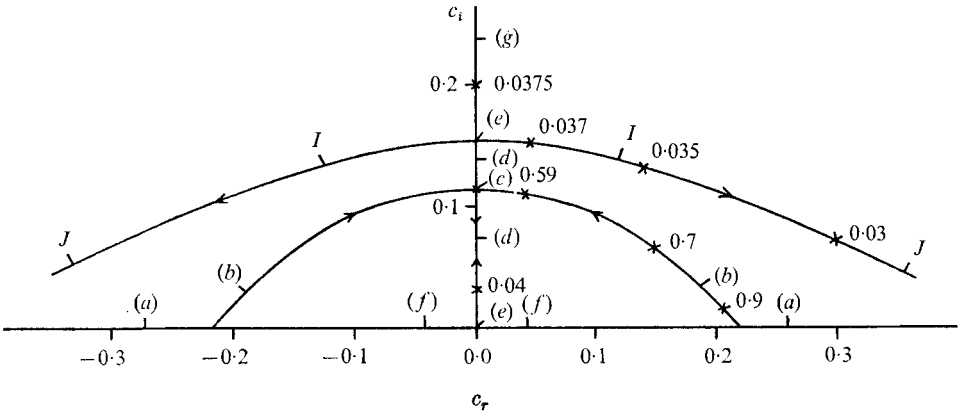

FIGURE 9. Locus of eigenvalues as a function of α for $u = \tanh(y)$, $\beta = \tanh(Ry)/R$, with $R = 5$, and $J = 0{\cdot}15$. Values of α are marked.

regions (*b*) and (*d*) are equal. (*f*) In this region, (and in (*g*)) there is one stationary, unstable mode. The dividing line between regions (*d*) and (*f*) is the stationary neutral curve (*e*). This relates to the other stationary, unstable mode, which is unstable *outside* it, in region (*d*). The programs cannot investigate its behaviour any further inside the neutral curve, but we know that it is neither unstable, nor neutral and stationary, so it is suspected that it is neutral and moving. The behaviour of the eigenvalues of c as α varies along a line of fixed J, passing through all the above regions, is shown in figure 9. The labels (*a*)–(*g*) correspond to the areas and lines of figure 8 (*b*).

3.13. *Discussion of results.* The results quoted above for the case $R = 5$ demonstrate that, even for fairly simple configurations, we cannot always expect simple stability characteristics. It must be emphasized that the stability boundaries and the curve of maximum growth in figures 8 (*a*), (*b*) are *not* accurate, but are merely extrapolations and deductions from the known eigenvalues. Because $Ri(\infty) = 0$, there is always a region where $Ri(y) < \frac{1}{4}$, for any value of J. Drazin & Howard (1966) discuss the results of Holmboe (1962) for the configuration

$$\left.\begin{aligned} u(y) &= \begin{cases} y/|y| & (|y| \geqslant 1) \\ y & (|y| \leqslant 1) \end{cases} \\ \beta(y) &= \begin{cases} \beta_\infty & (y > 0) \\ \beta_{-\infty} & (y < 0) \end{cases} \end{aligned}\right\} \quad (-\infty \leqslant y \leqslant \infty), \tag{3.7}$$

which is a piecewise continuous approximation to our present configuration with $R \gg 1$. The stability characteristics are very similar to those found for our con-

figuration (for $R = 5$). There is an unstable region where $c_r = 0$ near $J = 0$, and another unstable region, where $c_r \neq 0$, which extends to infinity. Near the origin the stability boundary is asymptotic to $J_0 = \alpha$, while both stability boundaries tend to $J_0 = \alpha - 1$ at infinity (see Drazin & Howard 1966, figure 7). The numerical values on the stability curves are different from those of figures 8(*a*, *b*). In particular, the instability for $J = 0$ is confined to $\alpha < 0{\cdot}64$, and the largest value of J for stationary unstable waves is less than 0·1. However, there is enough qualitative agreement to confirm the deductions we have made from our numerical results. We have shown that the flow is always unstable for some wavenumbers; but the growth rates are very small for large J, and the wavelengths are small too, so that in practice some sort of viscous damping is to be expected.

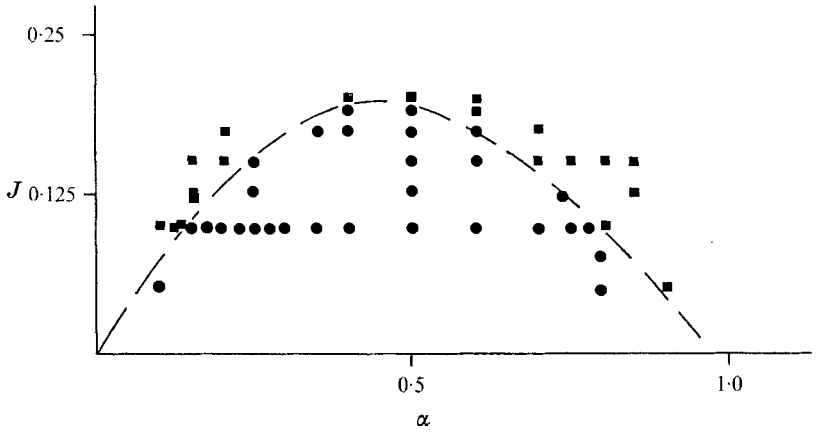

FIGURE 10. Stability characteristics for $u = \tanh(Qy)/Q$, $\beta = \tanh y$, with $Q = 1$ for $y \geqslant 0$, $Q = 1{\cdot}2$ for $y \leqslant 0$. ■, stable points; ●, unstable points.

3.14. *Effects of asymmetry.* A brief investigation into the effects of making the velocity profile slightly asymmetric was made. The profiles considered were

$$\left.\begin{aligned} u(y) &= \begin{cases} \tanh y & (\infty \geqslant y \geqslant 0) \\ (1/1{\cdot}2)\tanh(1{\cdot}2y) & (0 \geqslant y \geqslant -\infty) \end{cases} \\ \beta(y) &= \tanh y. \end{aligned}\right\} \tag{3.8}$$

Because of the asymmetry, only program (i) could be used here. It showed that the unstable modes for this configuration are moving ones, and that the stability boundary is not a stationary neutral curve, since the eigenvalues tend to non-zero real numbers on it. Figure 10 shows the stability boundary, drawn by plotting the stable and unstable points and then fitting the curve in between. Figure 11 shows the eigenvalues along a line of constant J, as α is varied, demonstrating the non-zero limits of c_r when c_i tends to zero. Here again, then, is evidence that slight changes in the configuration can radically alter the stability characteristics. In particular, it should be noted that the largest value of J for which there is instability is less than $\frac{1}{4}$.

These results are important, because few density or velocity profiles in the atmosphere or ocean are precisely symmetric. The effect of asymmetry is much

more noticeable in the phase speed c_r than in the growth rate αc_i for J less than 0·2. Thus, theoretical results obtained using symmetric profiles should be accurate when used to predict experimental growth rates in this region, but not when used for phase speeds.

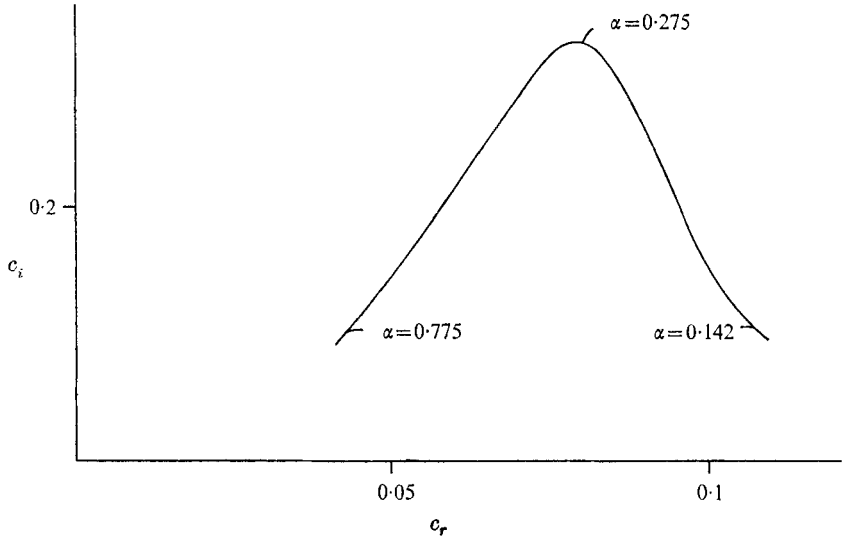

FIGURE 11. Locus of eigenvalues for $u = \tanh(Qy)/Q$, $\beta = \tanh(y)$, with $Q = 1$ for $y \geqslant 0$, $Q = 1{\cdot}2$ for $y \leqslant 0$, and $J = 0{\cdot}1$.

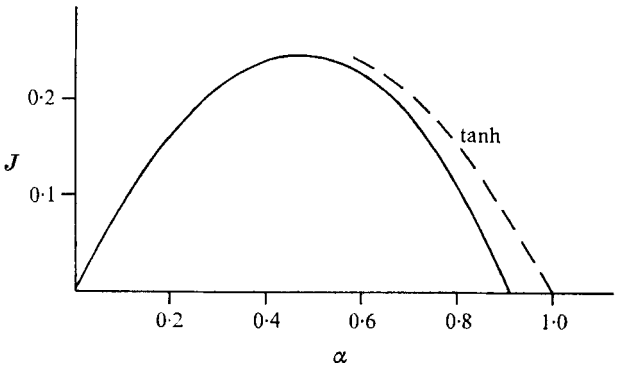

FIGURE 12. Neutral curve for error function profiles.

3.2. *The error function shear layer*

A better model than the hyperbolic tangent for experimental shear profiles is the error function. Previous authors have relied on theoretical results using hyperbolic tangent profiles to compare with experiment, because of the close approximation of $\tanh y$ to $\mathrm{erf}(\frac{1}{2}\sqrt{\pi}y)$, and the greater analytic simplicity of dealing with the hyperbolic tangent. In order to check the accuracy of the physical assumption that hyperbolic tangent and error function configurations were virtually identical in their stability characteristics, the following configuration was investigated numerically:

$$u(y) = \mathrm{erf}(\tfrac{1}{2}\sqrt{\pi}y), \quad \beta(y) = \mathrm{erf}(\tfrac{1}{2}\sqrt{\pi}y) \quad (-\infty \leqslant y \leqslant \infty). \tag{3.9}$$

It was found that the neutral curve and stability boundary for this configuration was indeed very close to that of the equivalent configuration using the hyperbolic tangent. It is shown in figure 12. A number of eigenvalues were also computed, and these, too, were not very different from the equivalent 'tanh' values. Thus, for most experimental purposes, the assumption of hyperbolic tangent profiles is sufficiently accurate.

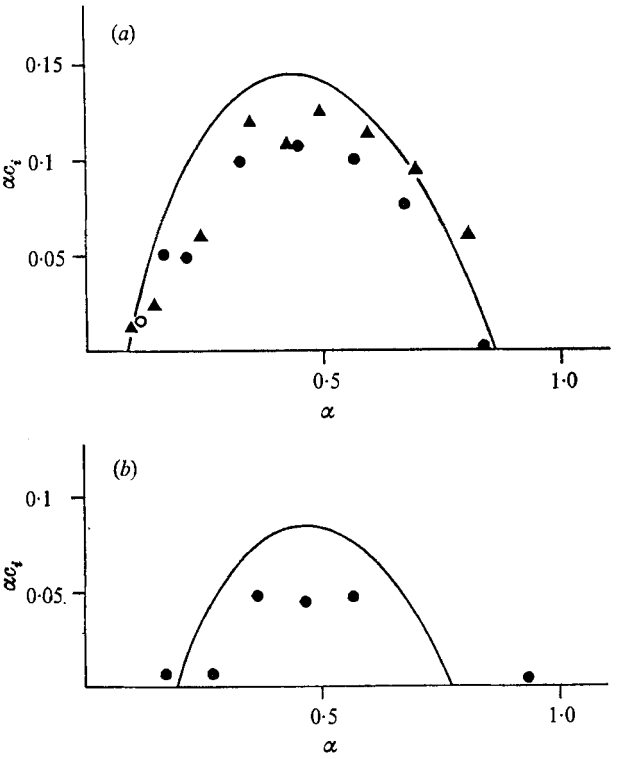

FIGURE 13. Comparison of growth rates for error function profiles with experiment; (*a*) $J = 0{\cdot}07$, (*b*) $J = 0{\cdot}15$.

3.21. *Comparison with experiment.* Scotti (1968) carried out experiments in a wind tunnel which investigated the stability of an error function shear layer made by allowing the interface between two streams of air, at different temperatures and velocities, to diffuse. Small disturbances were introduced into the interface and the resulting temporal growth rates of unstable waves were measured. The experimental profiles were such that the density scale of variation was slightly larger than that of the velocity; so, for comparison, we consider the following configuration:

$$u(y) = \operatorname{erf}(\tfrac{1}{2}\sqrt{\pi}y), \quad \beta(y) = (1/0{\cdot}8)\operatorname{erf}(0{\cdot}8\tfrac{1}{2}\sqrt{\pi}y) \quad (-\infty \leqslant y \leqslant \infty). \tag{3.10}$$

The comparison with experiment is shown in figures 13(*a*, *b*).† In figure 13(*a*), the circles and triangles represent two different experimental runs, while the

† Scotti used the density scale for his non-dimensionalization of the wavenumber α, whereas we have used the velocity scale, so his results as plotted here have all been multiplied by 0·8 to compare them with the numerical predictions.

solid line is drawn from computed values. The open circle is an experimental point which was actually measured as a decay rate, but has been plotted with its sign changed. There was only one run at the higher Richardson number (figure 13(*b*)). Almost all the experimental points fall inside the predicted curve, and this indicates that some form of damping was present in the experiments. The growth rates measured in the experiments were found to be dependent on the distance downstream from the disturbance at which they were measured, and "growth rates obtained at the mid and downstream stations were generally much smaller than those obtained upstream" (Scotti 1968). The upstream values are the ones used in figures 13(*a*, *b*), as Scotti gives an experimental explanation for the reduction of the growth rates downstream. This comparison between the experimental and the computed growth rates shows that inviscid, linear stability theory has some value in predicting the behaviour of the flow under the circumstances considered (cf. Thorpe 1969).

4. Channel profiles

4.1. *First configuration*

Three stationary neutral curves for the configuration

$$u(y) = \sin(y), \quad \beta(y) = y \quad (-\pi \leqslant y \leqslant \pi) \tag{4.1}$$

are given by Drazin & Howard (1966). Thorpe (1969) has pointed out that the third is in error. The correct forms are

$$J_0 = (1-\alpha^2)^{\frac{1}{2}} - 1 + \alpha^2, \tag{4.2}$$

$$J_0 = 3(1-\alpha^2)^{\frac{1}{2}} - 3 + \alpha^2 \quad (0 \leqslant \alpha \leqslant 1), \tag{4.3}$$

$$\alpha = \tfrac{1}{2}\sqrt{3}. \tag{4.4}$$

The second is satisfied only by negative J_0, and is of no interest in the present investigation. There is no analytic evidence as to whether either of (4.2) or (4.4) are stability boundaries, although the homogeneous flow ($J = 0$) is known to be stable for $0 \leqslant \alpha \leqslant \frac{1}{2}\sqrt{3}$.

Program (i) was used to investigate this configuration, and the results show that the neutral curve (4.2) is in fact a stability boundary for $0 \leqslant \alpha \leqslant \frac{1}{2}\sqrt{3}$, the remainder of the boundary being made up of the line $\alpha = \frac{1}{2}\sqrt{3}$ ($0 \leqslant J_0 \leqslant \frac{1}{4}$), which is part of the neutral curve (4.4). This is shown in figure 14, which also shows the curve of maximum growth. Figure 15 shows, for a point in the α, J plane near the curve of maximum growth, displacements of constant density lines in the central region of the flow.

4.2. *Second configuration*

Another configuration with $u = \sin y$ that was briefly considered was

$$u(y) = \sin(y), \quad \beta(y) = \tfrac{1}{2}y + \tfrac{1}{4}\sin(2y) \quad (-\pi \leqslant y \leqslant \pi). \tag{4.5}$$

The Brunt–Väisälä frequency is proportional to $\cos^2 y$, while the Richardson number distribution is constant, equal to J. Two stationary neutral curves are given by Thorpe (1969):

$$J_0 = \alpha^2(1-\alpha^2), \quad J_0 = \tfrac{3}{4} - \alpha^2. \tag{4.6), (4.7}$$

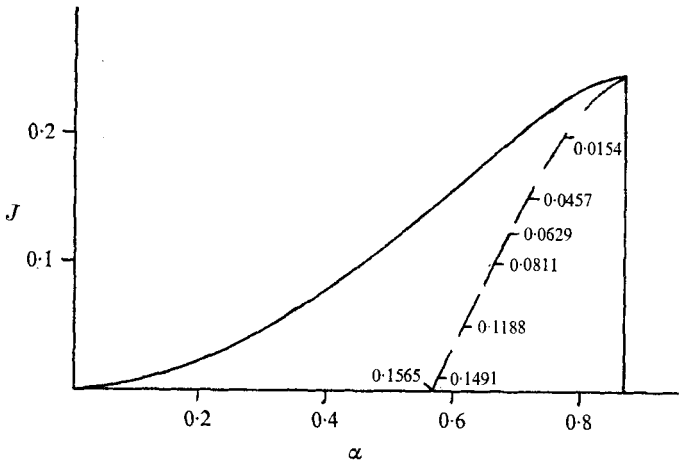

FIGURE 14. Stability boundary and curve of maximum growth for $u = \sin(y)$, $\beta = y(-\pi \leqslant y \leqslant \pi)$, with growth rates marked.

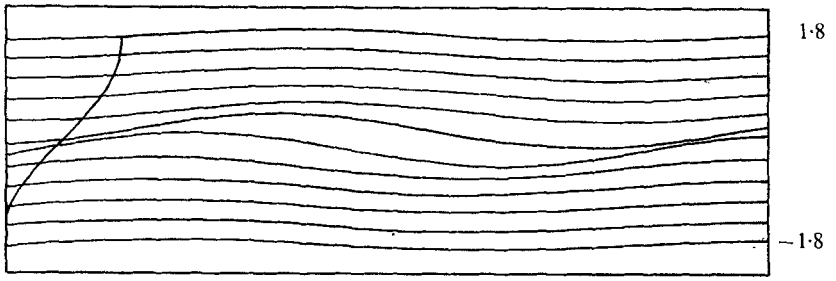

FIGURE 15. Displacement of dye lines in the flow $u = \sin(y)$, $\beta = y$, with $\alpha = 0{\cdot}6$, $J = 0{\cdot}01$.

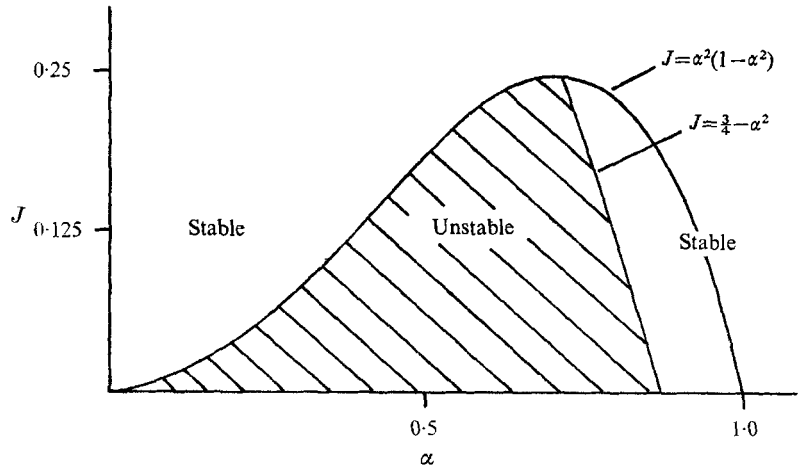

FIGURE 16. Stability boundary for the profiles $u = \sin(y)$, $\beta = \frac{1}{2}y + \frac{1}{4}\sin(2y)$.

In a similar way to the previous case, (4.6) is the stability boundary for

$$0 \leqslant \alpha \leqslant \sqrt{2},$$

while (4.7) is the stability boundary for $1/\sqrt{2} \leqslant \alpha \leqslant \frac{1}{2}\sqrt{3}$ (figure 16).

The above two configurations, besides modelling possible experimental situations, serve to illustrate complexities that can arise when there is more than one neutral curve.

5. Jet profiles

5.1. *The Bickley jet*

The profile $u(y) = \operatorname{sech}^2(y)$ is one of the standard forms used in modelling jet profiles; Drazin & Howard (1966) give neutral curves for two configurations. We shall consider the one with $N^2(y)$ constant. This is, on their scaling,

$$u^*(y) = \operatorname{sech}^2(y), \quad \beta(y) = y \quad (-\infty \leqslant y \leqslant \infty). \tag{5.1}$$

$u^*(y)$ is so called because it is not in the standard form used in this discussion. Note that it is not an odd function of y, and hence the unstable eigenvalues will *not* this time be found in pairs, $\pm c_r + ic_i$. Thus, the sign of c_r is important. The neutral curves given by Drazin & Howard are not stationary. They are given by

$$\left.\begin{aligned} J^* &= \alpha^2(4-\alpha^2)(9-\alpha^2)/225, \\ c^* &= (6+\alpha^2)/15, \end{aligned}\right\} \tag{5.2}$$

and

$$\left.\begin{aligned} J^* &= \alpha^2(1-\alpha^2)(9-\alpha^2)(3+\alpha^2)^2/9(3+5\alpha^2)^2, \\ c^* &= (3+\alpha^2)^2/3(3+5\alpha^2). \end{aligned}\right\} \tag{5.3}$$

There is no clear argument as to whether these are stability boundaries or not. The Richardson number distribution is

$$Ri^*(y) = J^*/4\operatorname{sech}^4 y \tanh^2 y. \tag{5.4}$$

The inflexion points are at $y = \pm y_0$, where $\tanh y_0 = 1/\sqrt{3}$. At these points the Richardson number achieves its minimum value, $(\frac{27}{16})J^*$. Thus, the use of J^* as a Richardson number for the flow is somewhat misleading!

In order to study this configuration numerically, we move the origin to the lower inflexion point, and normalize the profiles as in §1. Then (5.1) becomes

$$\left.\begin{aligned} u(y) &= (\operatorname{sech}^2(y-y_0) - \operatorname{sech}^2 y_0)/4\tanh^3 y_0, \\ \beta(y) &= y \quad (-\infty \leqslant y \leqslant \infty), \end{aligned}\right\} \tag{5.5}$$

where $\tanh y_0 = 1/\sqrt{3}$. The Richardson number distribution is

$$Ri(y) = 4J\tanh^6 y_0/\operatorname{sech}^4(y-y_0)\tanh^2(y-y_0); \tag{5.6}$$

it achieves its minimum value of J at $y = 0$ and $y = 2y_0$. The neutral curves (5.2) and (5.3) become

$$\left.\begin{aligned} J_0 &= 3\alpha^2(4-\alpha^2)(9-\alpha^2)/400, \\ c &= [(6+\alpha^2)/15 - \tfrac{2}{3}](\tfrac{3}{4}\sqrt{3}), \end{aligned}\right\} \tag{5.7}$$

and
$$\left.\begin{aligned} J_0 &= 3\alpha^2(1-\alpha^2)(9-\alpha^2)(3+\alpha^2)^2/16(3+5\alpha^2)^2, \\ c &= [(3+\alpha^2)^2/3(3+5\alpha^2)-\tfrac{2}{3}](\tfrac{3}{4}\sqrt{3}). \end{aligned}\right\} \tag{5.8}$$

The configuration cannot be studied using program (ii), as it does not satisfy the symmetry conditions. However, program (i) was used to find eigenvalues, and to

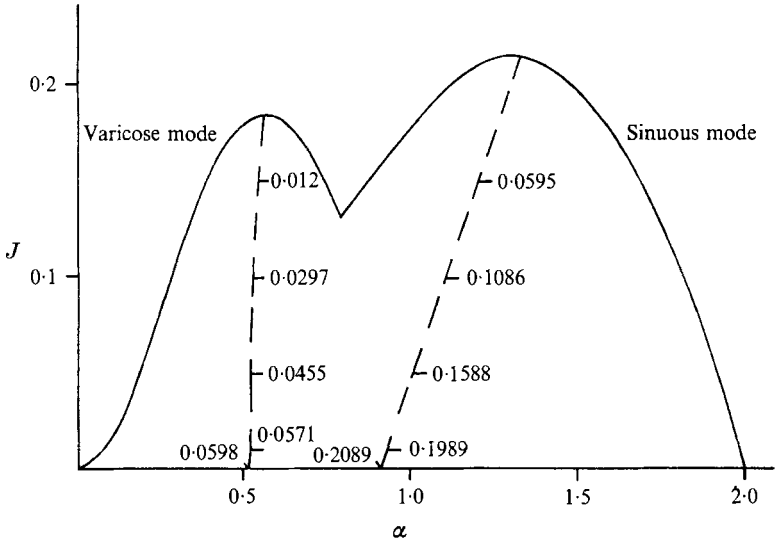

FIGURE 17. Stability boundary and curves of maximum growth for each mode for the Bickley jet with N^2 constant.

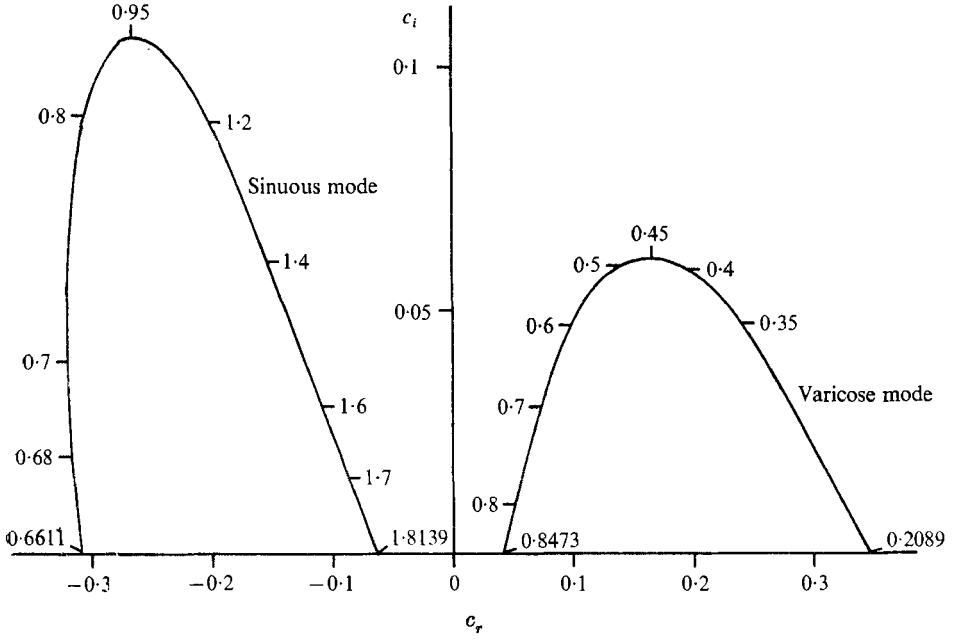

FIGURE 18. Eigenvalues for the Bickley jet with N^2 constant. $J = 0{\cdot}1$, while the α values are as marked.

test for stability. The growth rates found for the case $J = 0$ were found to be in complete agreement with Drazin & Howard's (1966) growth rates for a homogeneous Bickley jet. Further computations showed that the stability boundary for the whole flow is made up of the two upper sections of the curves (5.7) and (5.8) in the α, J plane, the unstable region being all the area included under either curve. This is shown in figure 17, which also shows the curves of maximum growth for each mode. This is another example where the stability boundary has its maximum below $J = \frac{1}{4}$. Equations (5.7) and (5.8) are each stability boundaries for their respective modes; this is revealed by studying the locus of eigenvalues

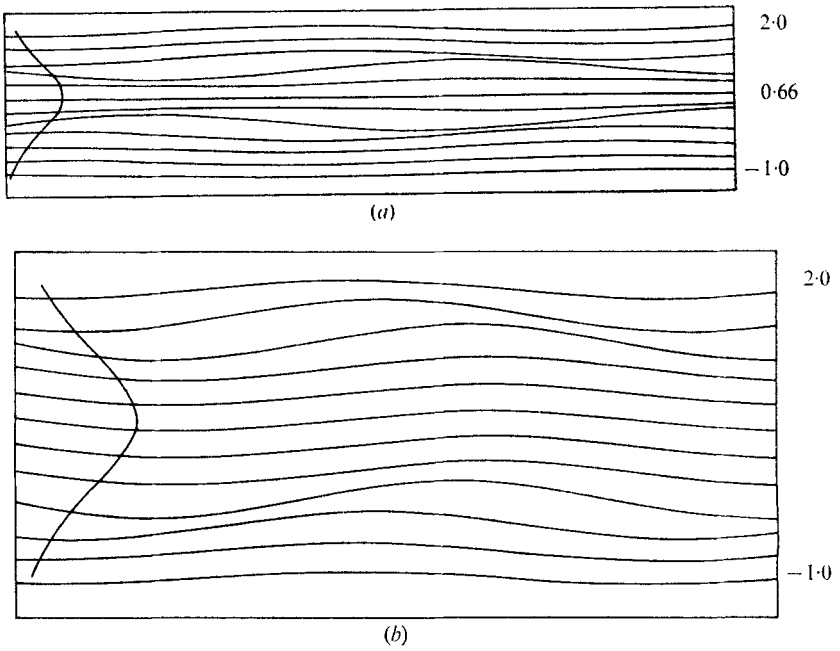

FIGURE 19. Displacement of dye lines in the Bickley jet with N^2 constant: (*a*) $\alpha = 0{\cdot}52$, $J = 0{\cdot}01$ (varicose mode); (*b*) $\alpha = 0{\cdot}9908$, $J = 0{\cdot}05$ (sinuous mode).

in the c plane along a line of constant J (see figure 18).† There is no evidence of a bifurcation point of the type found for the configuration (3.5). In this case, the two modes appear to be totally independent, one having $c_r > 0$, the other $c_r < 0$ (i.e. they travel in opposite directions). Figure 19 shows typical density line displacements for each mode. Relative to the inflexion point, the varicose disturbance moves forwards, and the sinuous one backwards ($c_r < 0$), so that relative to an origin chosen to make $u(y) = \operatorname{sech}^2 y$, the sinuous mode is the slower moving.

5.2. *The double jet*

The instantaneous velocity profile at the crest of a gravity wave on an interface between two fluids is $u(y) = \tanh y \operatorname{sech}^r y$, where r is related to the wave-

† In this figure, the values of c_r on the neutral curves (i.e. when $c_i = 0$) were computed from (5.7) and (5.8).

number. It is thus of interest to investigate the stability of this profile. We consider

$$u(y) = \tanh y \operatorname{sech}^r y, \quad \beta(y) = \tanh y \quad (-\infty \leqslant \infty \leqslant y). \tag{5.9}$$

The Richardson number distribution is

$$Ri(y) = \frac{J \operatorname{sech}^{2(1-r)} y}{(1-(1+r)\tanh^2 y)^2}. \tag{5.10}$$

For $r = 0$, we recover the configuration of Holmboe (1962), while $r = 1$ gives a case solved by Drazin & Howard (1966). For $0 < r < 1$, the Richardson number descends to zero at infinity, and can have a smaller value at the upper and lower inflexion points than it does at the central one. However, Ri has infinities between the origin and the other inflexion points, and these we expect to isolate the effects of the inflexion points from one another. Thus, we do *not* expect to find unstable moving modes of the type found for the hyperbolic tangent shear layer with small density scale.

Investigations using program (ii) revealed, as might be expected, that the stationary neutral curve changes smoothly from the $r = 1$ position to the $r = 0$ position as r varies from 1 to 0. Results from program (i) established that it remained the stability boundary throughout.

6. Conclusions

In §§3–5 we have considered a number of different configurations of density and velocity. We shall now summarize the results without reference to any particular profiles, and draw some general conclusions.

First, growth rates and curves of maximum growth have been computed for various configurations. Comparison with the experimental results of Scotti (1968) gives some agreement for shear-layer temporal growth rates, showing that the inviscid, linear stability analysis is useful for predicting the initial growth rates at high Reynolds number (within about 30 %, in most cases). No experimental results are available for any jet profiles.

Second, we have demonstrated the following.

(i) Long waves in a stratified shear layer where $Ri < \frac{1}{4}$ at the inflexion point are initially destabilized when the boundaries of the flow are brought in from infinity.

(ii) The major effect of asymmetry in shear-layer profiles is to alter the phase speed of the waves, without having much effect on the growth rates.

(iii) When there are two or more singular neutral modes, the stability boundary for the flow can be made up of parts of the corresponding neutral curves. The regions of stability and instability can often be guessed from a knowledge of the stability characteristics of the homogeneous flow with the same velocity profile.

(iv) The maximum value of the Richardson number for which some wavelength is unstable, in cases which exhibit instability, can be less than $\frac{1}{4}$. The actual values found, however, have not been less than 0·2 for all the unbounded velocity profiles (shear layers and jets) that have been considered. It would appear, therefore, that Miles's *necessary* condition for instability is quite a good *ad hoc*

sufficient criterion to use in the field. Nevertheless, most of the configurations have been smooth, symmetric profiles, which cannot be expected to model experimental situations precisely, so that due caution must be exercised.

(v) When the scale of the density variation is much less than that of velocity variation in a shear layer, the flow is unstable for some α, however large J may be. The unstable modes are moving ones for large J, but, in the region $0 \leqslant J < 0{\cdot}25$, they are stationary for some α, the dividing line being a locus of bifurcation points in the c plane. The stationary neutral curve marks an island of stability for one of the modes. It is of interest to know under what circumstances this type of instability (which we shall call type $\mathscr{D}$) can be expected. We might conjecture that a necessary condition is that Ri should tend to zero at infinity. There must also not be any infinities in $Ri(y)$ (e.g. as in profile (5.9)), as these will isolate the region near the origin from the effects of the small Ri at infinity. A stronger condition is that Ri should not have a local maximum, except at $y = 0$. A test of this conjecture is provided by the configuration

$$u(y) = \tanh y, \quad \beta'(y) = (1+\tanh^2 y)\operatorname{sech}^5 y \quad (-\infty \leqslant y \leqslant \infty), \tag{6.1}$$

which has a Richardson number distribution

$$Ri(y) = (1+\tanh^2 y)\operatorname{sech} y. \tag{6.2}$$

This function tends to zero at infinity, but has a minimum at $y = 0$. The stationary neutral curve was found using program (ii), and is only slightly different from the the case with $\beta = \tanh y$. Using program (i) to scan the α, J plane, no unstable modes were found outside the neutral curve.

Thus, we conjecture that instability of type $\mathscr{D}$ is to be expected for shear-layer configurations where the Richardson number is bounded, tends to zero at infinity, and has no local maximum except at the origin.

The work described in this paper forms the major part of the author's Ph.D. thesis (Hazel 1969). I am indebted to Dr F. P. Bretherton for a large amount of help and guidance while working on this problem, to Dr S. A. Thorpe for many fruitful discussions and suggestions, and to Dr H. Huppert for his help with the drafting of the original manuscript.

Appendix. Numerical solution of the eigenvalue problem

The eigenvalue problem is presented in terms of four parameters, α, J and the complex number c. It is convenient to regard two of the parameters as given, and to present results in the plane of the other two. There are then two obvious possibilities; find c given α and J, or find α and J given c. The former is a more local physical approach (viz. finding the growth rate and phase speed for completely specified profiles, considering a given wavenumber). The second possibility is useful when looking for stationary SNM's. In other cases, there is no guidance as to what values of c it is sensible to choose.

First program

The approach used in program (i) is to fix α and J, and to look for the eigenvalue c. As long as c_i is not zero, the equation is not singular, and, since we are looking for unstable solutions, this is always the case. A standard 'shooting' approach is used (i.e. we integrate the Taylor–Goldstein equation inwards, from the boundaries to the origin, then consider the matching problem across the origin). This technique has been used analytically by Drazin & Howard (1962), in solving the stability problem for long waves in a homogeneous shear flow, and numerically by Kaplan (1964) for a problem in laminar boundary-layer theory. For flows with boundaries at infinity, of course, it is impossible to start integrating actually at the boundaries. Since the boundary condition is $\phi = 0$, however, we expect ϕ to be exponentially decaying at $\pm\infty$. Writing (1.4) as

$$\phi' - \eta^2(y)\phi = 0, \tag{A 1}$$

we must require that $\eta^2(y)$ tends to a constant (possibly complex, but not on the negative real axis), as $y \to \pm\infty$, if we are to consider infinite flows. Then we can start the integration at $y = \pm Y$ say, where

$$|\eta^2(Y) - \eta^2(\infty)| \ll 1$$

in some appropriate sense, and take as the starting values of ϕ and ϕ', $\exp\{\mp\eta(y)y\}$ and $\mp\eta(y)\exp\{\mp\eta(y)y\}$ at $\pm Y$, respectively.†

The condition $\eta^2(y) \to$ constant at infinity is the only one placed on the velocity and density profiles, apart from those implicit in the non-dimensionalization. For flows in which the boundaries are not at infinity, the restriction on η^2 is unnecessary.

Thus, we integrate in from $\pm Y$ to the origin (keeping α and J fixed), to obtain ϕ_+, ϕ'_+ and ϕ_-, ϕ'_-(say) as the (complex) values of the numerical solutions and their derivatives at the origin. For a matched solution, we require ϕ and ϕ' to be continuous across the origin. Hence, we require

$$A\phi_+ = B\phi_- \quad \text{and} \quad A\phi'_+ = B\phi'_-,$$

where A and B are arbitrary constants. A solution is possible if $(\phi_+/\phi'_+) = (\phi_-/\phi'_-)$. We therefore define a matching function,

$$M(\alpha, J, c) = \phi_-\phi'_+ - \phi_+\phi'_-, \tag{A 2}$$

which is, of course, complex. The zeros of M as a function of c give the eigenvalues of c for fixed α and J. The special cases $\phi_+ = \phi'_+ = 0$ or $\phi_- = \phi'_- = 0$ were never found to occur in practice.

Program (i) evaluates the complex function $M(\alpha, J, c)$ at different points in the c plane (keeping α, J fixed and $c_i > 0$), and search for a point where $|M|$ is less than $|M|$ at all the surrounding points. When it has found such a point, it proceeds with a complex linear interpolation process in an attempt to find a zero of M. If the values of α and J are such that an unstable solution is possible, this process is found to converge very rapidly, giving an accuracy of 0·1 % for c in

† The square root of η^2 is chosen so that $-\frac{1}{2}\pi < \arg\eta < \frac{1}{2}\pi$.

three or four steps in most cases. Having found an eigenvalue, the program can then be made to output the full eigensolution for ϕ.†

If the values of α and J chosen are not such that an unstable solution is possible, then the program can find a solution only if the eigenvalue is such that c_r lies outside the range of $u(y)$. It cannot find neutral solutions with c_r inside this range, because the Taylor–Goldstein equation is then singular.

Second program

This program is much simplified in cases where $[\eta^2(y)]_{c=0}$ is an even function of y (i.e. when both $u(y)$ and $\beta(y)$ are odd functions), and, since a large number of interesting configurations satisfy these conditions, the program has been written for this case only. Keeping $c = 0$, the program looks for the corresponding eigenvalues of α and J. For profiles which satisfy the conditions of theorem (v), the stability boundary in the α, J plane is made up of neutral curves which are the loci of one or more stationary SNM's. Other neutral curves, in general, do not have c_r constant along their length. Whether or not a stationary neutral curve is a stability boundary can be established by investigating the eigenvalues near it, using program (i).

By definition, therefore, we put $c = 0$, and the Taylor–Goldstein equation becomes

$$\phi'' + \left\{\frac{J\beta'(y)}{[u(y)]^2} - \frac{u''(y)}{u(y)} - \alpha^2\right\}\phi = 0. \tag{A 3}$$

This is a real equation, which is singular at $y = 0$, since we have chosen our axes such that $u(0) = 0$. Thus, we can integrate in numerically only to within a non-zero distance of the origin, and the matching across the singular point must be achieved analytically. We do this by considering an approximate solution for $|y| \ll 1$. If we expand $u(y)$ and $\beta'(y)$ in Taylor series, the equation becomes, to highest order in each term,

$$\phi'' + \left\{\frac{J}{y^2} - \frac{2u_2}{y} - \alpha^2\right\}\phi = 0. \tag{A 4}$$

We can always choose $|y|$ small enough so that the y^{-2} term dominates. An approximate solution is then

$$\phi = \begin{cases} Ay^{\frac{1}{2}+\nu} + By^{\frac{1}{2}-\nu} & (J \neq \frac{1}{4}), \\ Ay^{\frac{1}{2}} + By^{\frac{1}{2}}\log y & (J = \frac{1}{4}), \end{cases} \tag{A 5}$$

where $\nu = (\frac{1}{4} - J)^{\frac{1}{2}}$, and A and B are arbitrary constants. In most of the cases we shall be considering, J will be less than or equal to $\frac{1}{4}$, but the analysis is not dependent on ν being real. Suppose now that we integrate (A 3) numerically inwards from the boundaries to points $y = \pm y_m$, such that $y_m \ll 1$, and (A 5) is a good approximation to the solution there. The starting values for the integration are determined as for program (i), but now, because $c = 0$, the equation is real. This means that $[\eta^2(\pm\infty)]_{c=0}$ must be a positive number. Suppose that the numerical values obtained from integrating inwards from the boundaries are

$$\phi_+, \phi'_+ \quad \text{at} \quad y = y_m,$$
$$\phi_-, \phi'_- \quad \text{at} \quad y = -y_m.$$

† The integration is carried out by means of a standard Runge–Kutta routine, using a variable steplength which is computed as $H(y) = 0{\cdot}1|\eta(y)|^{-1}$.

In the case where $[\eta^2(y)]_{c=0}$ is an even function, $\phi_+ = \phi_- = \phi$ (say), and $\phi'_+ = -\phi'_- = \phi'$ (say). Analysis similar to that for program (i) leads to a matching function

$$\mathscr{M}(\alpha, J) = J\phi^2 + y_m^2\phi'^2 - y_m\phi\phi'. \tag{A 6}$$

The zeros of $\mathscr{M}(\alpha, J)$ give the stationary neutral curve.

REFERENCES

Drazin, P. G. & Howard, L. N. 1962 *J. Fluid Mech.* **14**, 257.

Drazin, P. G. & Howard, L. N. 1966 *Advan. Appl. Math.* **9**, 1.

Goldstein, S. 1931 *Proc. Roy. Soc.* A **132**, 524.

Hazel, P. 1969 Ph.D. thesis, University of Cambridge.

Holmboe, J. 1960 Lecture Notes UCLA. (Unpublished.)

Holmboe, J. 1962 *Geophys. Publ.* **24**, 67.

Howard, L. N. 1961 *J. Fluid Mech.* **10**, 509.

Howard, L. N. 1964 *J. Mechanique*, **3**, 433.

Kaplan, R. E. 1964 *The Stability of Laminar Boundary Layers in the Presence of Compliant Boundaries.* U.S. Office of Naval Research.

Miles, J. W. 1961 *J. Fluid Mech.* **10**, 496.

Miles, J. W. 1963 *J. Fluid Mech.* **16**, 209.

Scotti, R. S. 1968 Ph.D. thesis, University of California, Berkeley.

Taylor, G. I. 1931 *Proc. Roy. Soc.* A **132**, 499.

Thorpe, S. A. 1969 *J. Fluid Mech.* **36**, 673.